Published in final edited form as:
Clin Cancer Res. 2009 November 15; 15(22): 6820–6829. doi:10.1158/1078-0432.CCR-09-1558.

Snail promotes CXCR2 ligand dependent tumor progression in NSCLC

Jane Yanagawa[1,2,5], **Tonya C. Walser**[1,2], **Li X. Zhu**[1,6], **Longsheng Hong**[1,3], **Michael C. Fishbein**[1,3], **Vei Mah**[3], **David Chia**[1,3], **Lee Goodglick**[1,3], **David A. Elashoff**[1,2,4], **Jie Luo**[1,2], **Clara E. Magyar**[3], **Mariam Dohadwala**[1,2,6], **Jay M. Lee**[1,5], **Maie A. St. John**[1,5], **Robert M. Strieter**[7], **Sherven Sharma**[1,6], and **Steven M. Dubinett**[1,2,3,6]

[1]Lung Cancer Research Program of the UCLA Jonsson Comprehensive Cancer Center, David Geffen School of Medicine at UCLA, Los Angeles, CA

[2]Department of Medicine, David Geffen School of Medicine at UCLA, Los Angeles, CA

[3]Department of Pathology and Laboratory Medicine, David Geffen School of Medicine at UCLA, Los Angeles, CA

[4]Department of Biostatistics, David Geffen School of Medicine at UCLA, Los Angeles, CA

[5]Department of Surgery, David Geffen School of Medicine at UCLA, Los Angeles, CA

[6]VA Greater Los Angeles Health Care Center, Los Angeles, CA

[7]Department of Medicine, University of Virginia, Charlottesville, VA

Abstract

Purpose—As a transcriptional repressor of E-cadherin, Snail has predominantly been associated with epithelial-mesenchymal transition (EMT), invasion, and metastasis. However, other important Snail-dependent malignant phenotypes have not been fully explored. Here, we investigate the contributions of Snail to the progression of non-small cell lung cancer (NSCLC).

Experimental Design—Immunohistochemistry was performed to quantify and localize Snail in human lung cancer tissues, and tissue microarray analysis (TMA) was utilized to correlate these findings with survival. NSCLC cell lines gene-modified to stably over-express Snail were evaluated *in vivo* in two severe combined immunodeficiency (SCID) murine tumor models. Differential gene expression between Snail over-expressing and control cell lines was evaluated using gene expression microarray analysis.

Results—Snail is up-regulated in human NSCLC tissue, and high levels of Snail expression correlate with decreased survival ($p<0.026$). In a heterotopic model, mice bearing Snail over-expressing tumors developed increased primary tumor burden ($p=0.008$). In an orthotopic model, mice bearing Snail over-expressing tumors also demonstrated a trend toward increased metastases. In addition, Snail over-expression led to increased angiogenesis in primary tumors as measured by MECA-32 ($p<0.05$) positivity and CXCL8 ($p=0.002$) and CXCL5 ($p=0.0003$) concentrations in tumor homogenates. Demonstrating the importance of these pro-angiogenic chemokines, the Snail-mediated increase in tumor burden was abrogated with CXCR2 blockade. Gene expression analysis also revealed Snail-associated differential gene expression with the potential to affect angiogenesis and diverse aspects of lung cancer progression.

Corresponding author: Steven M. Dubinett, M.D., Lung Cancer Research Program, Division of Pulmonary and Critical Care Medicine, 10833 Le Conte Avenue, 37-131 CHS, Los Angeles, CA 90095-1690, sdubinett@mednet.ucla.edu.

Disclosure of conflicts of interest: None

Conclusion—Snail up-regulation plays a role in human NSCLC by promoting tumor progression mediated by CXCR2 ligands.

Keywords

Snail; lung cancer; angiogenesis; CXCL8; CXCL5

Statement of Translational Relevance

Our study demonstrates for the first time the contributions of the transcriptional repressor Snail to lung cancer progression and suggests a potential pathway for new interventions. First, we show that high levels of Snail expression in human lung cancer specimens are associated with decreased survival, suggesting that Snail over-expression has a clinically significant effect. Second, we demonstrate that Snail over-expression leads to enhanced tumor growth in vivo, associated with increased angiogenesis and levels of angiogenic CXCR2 ligands, CXCL8 and CXCL5. Importantly, Snail-mediated tumor growth is abrogated with CXCR2 blockade. The connection between Snail and CXCR2 ligands introduces the manipulation of Snail expression as another pathway to influence the CXCR2 axis and tumor angiogenesis. Finally, gene expression profiling reveals that Snail over-expression affects a variety of malignant phenotypes, suggesting that targeting this pathway could simultaneously address diverse aspects of tumor progression and, ultimately, improve outcomes for patients with lung cancer.

Introduction

The number of deaths from lung cancer exceeds those from prostate, breast, colon, and pancreatic cancers combined, making lung cancer the number one cause of cancer mortality (1). Here, we investigate the contributions of the transcriptional repressor Snail to NSCLC progression, to identify a potential pathway for improved therapies.

SNAI1 (referred to as Snail) is a zinc-finger transcription factor made up of a highly conserved C-terminal region containing 4-6 zinc fingers, which serve as the DNA-binding domains that recognize consensus E2-box type elements (CAGGTG) (2). Snail transcriptionally represses the adherens junction protein, E-cadherin, by binding to these CAGGTG sequences within its promoter, ultimately inducing EMT (3). Both E-cadherin down-regulation and EMT have been implicated in tumor progression (4,5). Snail has also been found to play a role in the pathogenesis of several malignancies, predominantly enhancing invasiveness and metastatic behavior (6-10). However, recent studies suggest that Snail may play a broader role in carcinogenesis (11). For example, Kudo-Saito et al. (10) have shown that Snail up-regulation leads to tumor-promoting immunosuppression in melanoma. Snail up-regulation has also been associated with breast cancer recurrence (12) and resistance to therapies (13-15).

A few studies have suggested that Snail may also play a role in NSCLC tumor progression. Dohadwala et al. (16) demonstrated that PGE2 up-regulated Snail in a NSCLC cell line (A549), while Zhuo et al.(17) showed that Snail knock-down in A549 increased sensitivity to cisplatin. However, the importance of Snail in lung cancer remains incompletely explored. Here, for the first time, we demonstrate Snail up-regulation and its correlation with prognosis in NSCLC. In addition, *in vivo* studies utilizing Snail over-expressing NSCLC cell lines suggest that Snail promotes tumor progression and angiogenesis mediated by the CXCR2 ligands, CXCL8 and CXCL5.

Materials and Methods

Immunohistochemistry

Sections were obtained from human lung cancer specimens archived in the UCLA Lung Cancer SPORE tissue bank (IRB#02-07-011). Antigen retrieval was accomplished with either sodium citrate 10 mM pH 6.0 (Snail and E-cadherin) or EDTA pH 8.0 (Ki67). For single staining, sections were blocked with 10% normal goat serum, then probed with an antibody against Snail (ab17732, Abcam, Cambridge, MA) using a working dilution of 1:500 for tissue staining and 1:1600 for cell pellet staining or with an antibody against Ki67 (M7240, Dako, UK) using a working dilution of 1:200. Primary antibodies were incubated overnight at 4°C. After incubation with secondary antibody (Vector Laboratories, Burlingame, CA, USA), staining was developed using DAB Substrate Kit for Peroxidase (SK-4100, Vector Laboratories). For co-staining, sections were probed with Snail antibody (1:500) in 0.5% casein. Secondary antibody (K4003, Dako) was added and developed with DAB. Next, sections were incubated with E-cadherin (1:50) in 2% BSA overnight at 4°C. Sections were treated with an alkaline phosphatase standard (AK-5000, Vector) and developed with an alkaline phosphatase substrate kit (SK-5100, Vector). Counter-stain was achieved with hematoxylin. To create cell pellets, cells were incubated in 10% formalin for 6 hours, re-suspended in 2% agarose, and paraffin-embedded. For the blocking peptide control, sequential tissue sections were stained with Snail antibody (1:500 df) alone or Snail antibody (1:500 df) that had been previously reacted with snail blocking peptide (ab19126, Abcam)(1μg/mL) for 30 minutes, per manufacturer's instructions. Snail expression was evaluated by a pathologist (MCF) specializing in cardio-pulmonary disease. Evaluation of tumors, histologically normal airways, and alveolar epithelium was based on two criteria - intensity and percent positivity. For intensity: Grade 0 (no staining) to Grade 4 (most intense staining). For percent positivity: Grade 1 – 1-25%, Grade 2 – 26-50%, Grade 3 – 51-75%, Grade 4 – 76-100%. To compare areas of evaluation, we multiplied the intensity and percent positivity grades for each area to derive single values that represented both characteristics. Photomicrographs were obtained using an Olympus BX50 microscope, with Plan APO objective lenses. An Olympus DP11 camera and Olympus Camedia software were used to produce the images.

To quantify Ki67 staining, slides were analyzed using the Ariol SL-50 automated slide scanner (Applied Imaging, San Jose, CA). Thresholds for each image were applied using the Ariol analytical software based on multiple parameters: RGB algorithm, shape and size. All analyses were performed with the MultiStain script. Individual cells were discriminated by incorporating the shape, size, and thresholds to provide actual cell counts. Total tissue area analyzed was also included in the final analysis. Images were obtained with Aperio ImageScope software.

Lung Tissue Microarray

TMA was constructed using UCLA Department of Pathology archival paraffin-embedded lung samples from consecutively accrued cases that were obtained under appropriate IRB and HIPAA regulations. The characteristics of this TMA have been previously described (18) and are represented in detail in Supplemental Table 1. Snail-stained lung TMA was scored on a semi-quantitative basis by a board-certified pathologist (VM) blinded to clinical information. Nuclear Snail staining was quantified based on the percentage of cells staining, similar to previously described methods (18). The range of Snail expression was 0 - 100% integrated intensity (i.e., a measure of frequency (F) and intensity (I); FxI). Therefore, Snail expression was a continuous variable. The cut-point of 75% was determined by using recursive partitioning combined with regression trees (rpart package) and plotting log-rank P values versus hazard ratios. This provided optimal points of dichotomization. Extensive internal validation was performed to guard against data overfitting (19,20).

Cell lines

The lung cancer cell lines used in this study, H441 (adenocarcinoma), H1437 (adenocarcinoma), and H292 (mucoepidermoid), were obtained from American Type Culture Collection (Manassas, VA). Cells were stably transduced as follows: wild-type Snail cDNA pcDNA3 (a gift from Dr. E. Fearon, University of Michigan) was excised from the plasmid with HindIII and EcoRV and subcloned into the retroviral vector pLHCX (Clontech, Mountain View, CA), which includes a drug resistance (hygromycin B) marker. All constructs were verified by restriction endonuclease digestion. For virus production, 70% confluent 293T cells were co-transfected with pLHCX-Snail or pLHCX (vector alone). Tumor cells were then transduced with high-titer supernatants producing either Snail or pLHCX virus. Following transduction, the tumor cells were selected with hygromycin B. Cells were verified by genotyping and tested for mycoplasma. The following cell line terminology was used: H441S, H1437S, and H292S represent Snail over-expressing cell lines. H441V, H1437V and H292V represent corresponding vector control cell lines.

Growth conditions

For 2-dimensional cell cultures, cells were grown in RPMI 1640 with L-glutamine (Cellgro, Manassas, VA), supplemented with 10% FBS (Gemini Bioproducts, West Sacramento, CA), 1% penicillin-streptomycin (Gibco-Invitrogen, Carlsbad, CA) and 350μg/mL hygromycin B (Hyclone, Logan, UT). For three-dimensional spheroid culture (21), 12-well plates were coated with 250 μL Engelbreth-Holm-Swarm (EHS) extracellular matrix extract, growth-factor reduced, (Trevigen, Gaithersburg, MD). Plates were then incubated at 37°C for 30 minutes. 75,000 cells were added to each well in 500 μL of growth medium with 5% EHS. This growth medium was replaced every three days. Cells were maintained at 37°C with 5% CO_2. Photomicrographs were produced using a Leica DM IRB microscope, and Olympus America Magnafire digital camera and software.

Western blots

Western analysis was performed as previously described (16). Protein concentrations were derived using a BCA protein assay kit (Pierce, Rockford, IL) per kit instructions, and read on a Bio-rad Benchmark plate reader (Hercules, CA). Membranes were blocked with 5% Blotto non-fat dry milk (Santa Cruz, Santa Cruz, CA). For Snail (20μg), membranes were incubated with antibody (SN9H2, Cell Signaling, Danvers, MA) at 1:1000 overnight at 4°C, and developed with Western Lightning Plus-ECL (NEL105001EA, Perkin Elmer, Waltham, MA). For E-cadherin (20μg), membranes were incubated with antibody (610182, BD Transduction Laboratories, San Jose, CA) at 1:10000 overnight at 4°C, and developed with Super Signal West Pico Chemiluminescent Substrate (34080, Thermo-Scientific, Waltham, MA).

NSCLC tumor growth in SCID mice

Pathogen-free SCID Beige CB17 female mice, 6-12 weeks of age, were obtained and maintained at the West Los Angeles VA Animal Research vivarium. All studies were approved by the institution's animal studies review board. For the heterotopic model, 5×10^6 cells of each NSCLC cell line were implanted subcutaneously into the left flank of each mouse. Tumor growth was assessed three times a week. Two bisecting diameters of each tumor were measured with calipers, and volume calculated using the formula $0.4\times ab^2$, where a represents the longer diameter and b the shorter diameter. At the time of harvest, primary tumors were homogenized in lysis buffer with protease inhibitors (Tissue Extraction Reagent I, FNN0071, Invitrogen). Tumor lysates were cleared of insoluble debris by centrifugation to produce homogenates for ELISA analyses. For the orthotopic model, 1×10^4 cells in 25μl normal saline were injected via a small posterior transthoracic incision into the left lung, utilizing a tuberculin syringe with a 30-gauge needle. For CXCR2 blocking experiments, polyclonal goat anti-murine CXCR2

antibody was produced by the immunization of a goat with a peptide containing the ligand-binding sequence Met-Gly-Glu-Phe-Lys-Val-Asp-Lys-Phe-Asn-Ile-Glu-Asp-Phe-Phe-Ser-Gly (gift from Dr. Robert Strieter's lab). Mice were treated with 0.5 ml of the anti-CXCR2 antibody or control antibody (normal goat serum, G6767, Sigma-Aldrich, St. Louis, MO) via intraperitoneal injections, five times a week starting one day after tumor inoculation.

Flow cytometry

To analyze intratumoral vessel-formation, single-cell suspensions of xenograft primary tumors were evaluated with anti-MECA-32 antibody (553849, BD Bioscience) and isotype control (553927, BD Bioscience). To analyze incidence of metastases, multiple organs were evaluated with a CD49b antibody (555498, BD Pharmingen). A total of 10,000 gated events were analyzed on a BD FACScan flow cytometer using CellQuest software.

ELISAs for angiogenic factors

Levels of human CXCL8 and CXCL5 were quantified in primary tumor homogenates using sandwich ELISA kits (DY208 and DY254) purchased from R&D Systems (Minneapolis, MN), per kit instructions. The A450nm was determined by Vmax Kinetic microplate reader (Molecular Devices, Sunnyvale, CA).

Proliferation Assays

For the comparison of *in vitro* proliferation rates, cells were plated 1500 cells/well (6 well replicates) in 96-well plates with 100 μL/well of growth medium. ATP luminescence assay (ATPLite 1step Luminescence Assay Kit, Perkin-Elmer) was performed, per kit instructions, on one set of plates after 24 hours to obtain a baseline reading for the different cell lines, and read in a FLx800 microplate reader (Bio Tek, Winooski, VT) using KCjunior for Windows Data Reduction Software (Bio Tek). Subsequent plates were read at 48, 72, and 96 hours, and results were divided by the corresponding baseline readings (24 hour) to provide fold-change with time.

Differential gene expression analysis

Single samples of RNA were collected with Qiagen RNeasy Mini kit (Qiagen, Valencia, CA). Differential gene expression was evaluated using Affymetrix Gene Chip Human Genome U133 Plus 2.0 arrays. Harvard dChip software (22) was used for data analysis, and key findings were validated by western analysis. For Table 1 and Supplemental Table 1, overall differential expression was analyzed by comparing vector and Snail over-expressing cell lines in aggregate, using the following criteria: fold change >1.1, absolute change between groups >20, percent of probe sets called present > 20%, and paired t-test p-value <0.05. To account for heterogeneity among parental cell lines, Supplemental Table 2 represents probe sets substantially altered (>10 fold) in at least one paired cell line. Microarray data discussed in this publication are deposited in NCBI's Gene Expression Omnibus (GEO Series accession number GSE16194).[1]

Statistics

To compare staining between tissue types, proliferation rates between cell lines, as well as tumor weights and analyses (flow cytometry and ELISA) between murine experimental groups, p-values were generated using the Wilcoxon test (rank sum or signed rank as appropriate) or Student's t-test. To compare tumor growth curves between murine experimental groups, analysis of variance (ANOVA) models were constructed for each experiment, using tumor

[1] http://www.ncbi.nlm.nih.gov/geo/query/acc.cgi?acc=GSE16194

volume as the outcome. These models included effects for group, time, and the group by time interaction effect. For the CXCR2 experiment, an overall ANOVA model was performed prior to post-hoc comparisons between individual groups. For TMA analysis, statistical and pooling criteria have been previously described (18). For dichotomized (high versus low) nuclear Snail expression, survival curves were calculated using the Kaplan-Meier method and comparisons performed using the log-rank test. The optimal dichotomizing cut-point was found to be at the 75th percentile of lung cancer tissue staining and was determined using a recursive partitioning regression tree (23) followed by plotting the log-rank p-values versus the hazard ratios. Analyses were conducted using SOCR[2] and R version (2.8)[3]. P-values were two-sided and $p < 0.05$ considered significant.

Results

Snail is up-regulated in human NSCLC tissues

Immunolocalization of Snail in paraffin-embedded lung adenocarcinoma (n=11) and squamous cell carcinoma (SCC) (n=9) revealed increased expression in tumors as compared to surrounding histologically normal lung tissue (Figure 1*A*). Occasional Snail staining also appeared in lymphocytes, normal airway, and alveolar epithelium. Snail staining of a paraffin-embedded agarose pellet composed of H441V cells as compared to a H1437S pellet revealed differential staining at 1:1600, serving as negative and positive controls, respectively. Staining was absent in the human NSCLC tissue isotype control sample. Snail blocking peptide effectively inhibited staining in adenocarcinoma as well as SCC tissues (Supplemental Figure 1). Snail staining was evaluated to compare expression between tumors and surrounding normal tissues (Figure 1*B*). Significant differences were established between tumors and normal airways, as well as between tumors and normal alveolar tissue ($p<0.05$). No significant difference was noted when comparing adenocarcinoma with SCC tissue staining. Co-staining was also performed with these NSCLC specimens (n=18), revealing a non-uniform pattern of membranous E-cadherin staining in the presence of nuclear Snail staining (Figure 1*C*). In regions of more poorly-differentiated and infiltrative tumor, there tended to be less E-cadherin expression. In addition, there was more E-cadherin in the central regions of SCC tumors than at the invasive edges adjacent to normal lung tissue. This pattern of expression was not apparent in the adenocarcinomas. TMA of 237 lung adenocarcinomas revealed significantly decreased survival for patients with tumors that exhibited higher levels of Snail expression (Figure 1*D*). Analysis of 104 lung SCC specimens did not reveal a significant difference in prognosis (data not shown).

Snail over-expression leads to morphologic changes in NSCLC cell lines

Western blot analysis verified elevated levels of Snail with a corresponding down-regulation of E-cadherin in NSCLC cell lines stably transduced to over-express Snail (Figure 2*A*). In two-dimensional culture, Snail over-expressing cells were characterized by a more spindle-like morphology, larger size, and increased space between cells (Figure 2*B*). Growth in three-dimensional spheroid culture revealed phenotypic differences between H441S as compared to H441V (Figure 2*C*). H441V formed large, cohesive spheroids, while H441S formed smaller, markedly discohesive spheroids.

Snail over-expression promotes NSCLC tumor progression *in vivo*

To determine whether Snail over-expression modulates NSCLC tumor growth *in vivo*, we utilized a heterotopic (subcutaneous) SCID mouse tumor model. With the implantation of

[2]http://socr.ucla.edu
[3]www.r-project.org

either H441V/H441S or H292V/H292S cells, growth curves measuring tumor volume over time were significantly different (both group and interaction effects $p<0.001$) between Snail over-expressing tumors and vector control tumors. Ultimately, mice bearing Snail over-expressing tumors developed a significant increase in primary tumor burden ($p=0.008$) as compared to mice bearing vector control tumors (Figure 3*A*/*B*). To determine whether Snail over-expression influences NSCLC metastases *in vivo*, we used an orthotopic (transthoracic) SCID mouse tumor model. Metastases were quantified by flow cytometry gated on CD49b (human marker) expressing tumor cells. Although not reaching statistical significance, we found a trend towards increased metastases to the contralateral lung, liver, bone marrow, and adrenal glands in mice bearing H441S tumors (Figure 3*C*). Similar trends were observed with the orthotopic implantation of H1437V/H1437S. Using the heterotopic model, the incidence of hepatic and pulmonary metastases had also been evaluated and was found to be elevated in mice bearing H441S as compared to H441V (data not shown).

Snail over-expression is associated with increased proliferation *in vivo* but not *in vitro*

To investigate the Snail-mediated increase in tumor burden, H441V/H441S primary tumors harvested from the heterotopic model were evaluated by immunohistochemistry for the proliferation marker, Ki67. Results revealed a significant elevation ($p<0.05$) in Snail over-expressing tumors (Figure 4*A*). In contrast, using an *in vitro* proliferation assay, two of three Snail over-expressing cell lines exhibited a highly significant proliferative disadvantage as compared to their paired vector control cell line (Figure 4*B*). ($p<0.008$)

Snail over-expression leads to increased vessel formation and elevated levels of angiogenic factors, CXCL8 and CXCL5

At the time of harvest, it was noted that Snail over-expressing tumors were grossly more vascularized. To determine whether the increase in tumor growth was associated with increased angiogenesis, primary tumors were evaluated by flow cytometry gated on the murine endothelial cell surface marker, MECA-32. Levels were significantly elevated in the Snail group (Figure 4*C*). To assess angiogenic factors, primary tumor homogenates were also analyzed by ELISA for human CXCL8 and CXCL5. Levels of both angiogenic factors were significantly increased in the H441S tumors (Figure 4*D*). ($p<0.05$) Similar results were found with H292S tumors (data not shown). In contrast, analysis by western blot, multiplex, and ELISA failed to show consistent elevation of either CXCL8 or CXCL5 in Snail over-expressing cell lines *in vitro* (data not shown). The increase of CXCR2 ligands observed *in vivo* may depend on interactions between Snail over-expressing cells and the tumor microenvironment, which are not represented *in vitro*. Previous reports also support a critical role for the tumor microenvironment in the induction of CXCR2 ligands (24, 25). In addition, our findings are well-supported by the results of several studies in the literature documenting that levels of these CXCR2 ligands are elevated in human non-small cell lung cancer specimens and correlate with poor survival (26-28).

Snail-dependent tumor growth is abrogated by CXCR2 blockade

To evaluate the extent to which the Snail-mediated increase in proliferation and tumor burden was dependent on elevated levels of CXCL8 and CXCL5, we treated mice bearing H441S tumors with an antibody that neutralizes CXCR2, the receptor for both CXCL8 and CXCL5. Untreated H441S tumors grew significantly larger than H441S tumors treated with CXCR2 blockade ($p<0.03$). In fact, treatment with anti-CXCR2 antibody resulted in H441S tumors with growth curves and weights equivalent to those of H441V tumors (Figures 5*A*/*B*). The overall comparison of growth curves for the four experimental groups (H441V, H441S untreated, H441S treated with control antibody, H441S treated with CXCR2 antibody) had significant group and interaction effect ($p<0.001$). When examining groups in pairs, all pairs

had significant group and interaction effects ($p<0.001$) except for H441V versus H441S treated with CXCR2 blockade and H441S untreated versus H441S treated with control antibody.

Snail over-expression is associated with differential gene expression related to diverse aspects of lung cancer progression

To evaluate the global effects of up-regulated Snail, gene expression analysis was performed on Snail over-expressing cell lines and corresponding vector control cell lines. dChip analysis revealed differential gene expression affecting diverse aspects of lung cancer progression, including angiogenesis, invasion, cell cycle regulation, and the inhibition of tumor suppression (Table 1). Complete gene lists for two methods of analysis are provided in Supplemental Tables 2 and 3.

Discussion

Several studies demonstrate the importance of EMT and decreased E-cadherin in NSCLC, but the specific contributions of Snail to the progression of this disease have not been fully explored. Here, we describe a role for Snail in NSCLC progression, demonstrating that 1) Snail levels are elevated in human NSCLC tissue samples and correlate with decreased survival, 2) Snail over-expressing NSCLC cell lines yield larger tumors *in vivo* with enhanced angiogenesis and elevated levels of the angiogenic factors, CXCL8 and CXCL5, and 3) when the activity of these chemokines is blocked with an anti-CXCR2 antibody, the Snail-mediated increase in tumor growth is abrogated.

Immunolocalization of Snail in human lung cancer tissues reveals important implications. First, Snail is significantly up-regulated in NSCLC tissues and high expression is associated with poor prognosis. This correlation is consistent with the consequences of Snail over-expression as described in our *in vitro* and *in vivo* results, including increased angiogenesis, E-cadherin down-regulation, and elevated levels of CXCR2 ligands. In fact, each of these events has been previously shown to be associated with poor prognosis in NSCLC (27,29,30), suggesting that manipulation of Snail may be a novel approach to addressing these downstream events. Secondly, immunohistochemistry localizes Snail protein to the nucleus in NSCLC tissues. Post-translational mechanisms have been determined to control Snail activity by regulating its stability and subcellular localization. For example, GSK-3β phosphorylation of the Snail nuclear export signal and destruction box induces its cytoplasmic export and ubiquitin-mediated proteasomal degradation (31). On the other hand, interaction with the inflammatory microenvironment leads to NFkappaB-mediated nuclear stabilization of Snail (32). In this study, Snail maintains a nuclear presence, suggesting that it is transcriptionally active in the setting of NSCLC. This is further supported by our gene expression analysis of Snail over-expressing and vector control cell lines, which revealed differential profiles suggesting that Snail promotes diverse malignant phenotypes. Finally, although transcriptional repressors are expressed at the invading edge in the classic model of EMT-mediated tumor progression (33, 34), Snail staining appears throughout the tumor, with more pronounced repression of E-cadherin at the invading edge. This E-cadherin gradient was more apparent in SCC, but was also associated with more infiltrative and poorly differentiated regions in both SCC and adenocarcinomas. These results are consistent with reports that demonstrate a variable relationship between Snail and E-cadherin levels in other malignancies (35,36). Mechanisms by which this phenomenon occurs likely involve interactions with the tumor microenvironment (2) and may reflect interplay with other transcription repressors (ZEB1 (37) and Slug (38) have also been suggested to play a role in NSCLC), as well as regulation of co-repressors in the Snail chromatin-remodeling complex (39). These interactions are important areas of study in the investigation of EMT in tumor progression, and their relationship with Snail in the context of NSCLC deserves further investigation.

In addition, our *in vivo* and *in vitro* findings shed light on how Snail promotes tumor progression in NSCLC. In the current studies, Snail over-expressing cell lines do not demonstrate a proliferative advantage *in vitro*. Other studies have described similar results including Snail-mediated induction of partial cell cycle arrest (2,40,41). This is consistent with our findings; Snail over-expressing cell lines reveal differential gene expression of cell cycle-related genes (Table 1). Yet, the growth of Snail over-expressing cells *in vivo* leads to significantly increased tumor burden, suggesting enhanced tumor growth is mediated by an interaction with the tumor microenvironment. Specifically, we determined that Snail over-expression leads to the induction of angiogenesis, which is considered to be among the most crucial interactions between tumor and stroma in cancer progression (42). Angiogenesis occurs when the balance of angiogenic and angiostatic factors is disrupted. Gene expression analysis demonstrates that a number of such antagonizing signals are differentially expressed in Snail over-expressing cell lines. *In vivo*, the ultimate effect of this imbalance is increased vascularity and tumor progression associated with the expression of CXCR2 ligands.

CXC chemokines are a family of both angiogenic and angiostatic peptides. Angiogenic peptides possess a glutamic acid-leucine-arginine (ELR) motif and are bound by a single receptor, CXCR2. The interaction of ELR^+CXC ligands (such as CXCL5 and CXCL8) with endothelial CXCR2 leads to the induction of angiogenesis, and a strong body of literature now suggests that the CXCR2 axis is important in human lung cancer (43). Both CXCL8 (44)and CXCL5 (26) are elevated in human NSCLC, and a role for these ligands in the *in vivo* development of inflammation, angiogenesis, and neoplasia has been described (45,46). In addition, CXCR2 depletion with the use of a neutralizing antibody has been shown to decrease vascularity in a murine tumor model of NSCLC (45), as well as to inhibit the progression of premalignant alveolar lesions and induce apoptosis of vascular endothelial cells within alveolar lesions in $KRAS^{LAI}$ mice (46). Using an *in vitro* model of lung carcinogenesis that included both normal and immortalized bronchial epithelial cells as well as NSCLC cell lines, Sun et al. (25) also found that the expression of CXCR2 ligands directly correlated with progression from normal to premalignant to a highly invasive phenotype. Of note, in our evaluation of angiogenic factors, we also found that levels of VEGF were elevated in Snail over-expressing tumors. Despite elevated levels of VEGF, CXCR2 blockade led to reversal of the tumor growth advantage associated with Snail over-expression in the xenograft model, highlighting the significance of the CXCR2 axis. Similar findings in the simultaneous evaluation of CXCR2 ligands and VEGF have been reported in the literature. For example, Mizukami et al. (47) demonstrated that knockdown of tumor cell-derived HIF-1α markedly inhibited the expression of VEGF in tumors, without eradicating tumor-associated angiogenesis. The study further suggested that this was a result of reactive oxygen species and subsequent NFkappaB activation with the induction of angiogenic ELR^+ CXC chemokine CXCL8. IL-1β can induce angiogenic ELR^+ CXC chemokines (as well as VEGF) and consequent angiogenesis in NSCLC (25). The angiogenic effect produced by IL-1β was reversible with blockade of CXCR2, but not with anti-VEGF treatment (25). These and other recent studies suggest that manipulation of the CXCR2 axis --via pathways that may be dependent or independent of VEGF -- may be an important element of future anti-angiogenic strategies. Similarly, CXCL8 has been shown to control VEGF expression in endothelial cells, suggesting that CXCR2 blockade may have a downstream anti-VEGF effect (48). In support of these pre-clinical studies, a clinical study by Schultheis et al (49) also suggests that CXCL8 and CXCR2 single nucleotide polymorphisms contribute to resistance to anti-VEGF therapy. In fact, a recent preliminary report demonstrated that CXCR2 SNPs were among the genetic variants associated with clinical outcomes in NSCLC patients treated with bevacizumab (50). These studies imply that the CXCR2 axis may also serve as a VEGF-independent pathway that compensates for the loss of VEGF and mediates sustained tumor angiogenesis.

In summary, we demonstrate for the first time that Snail is up-regulated in human NSCLC and is associated with decreased survival. In addition, Snail over-expression promotes increased angiogenesis and tumor progression mediated by the CXCR2 axis in murine lung cancer models. Further investigations should provide insight into the regulation of Snail and Snail-dependent malignant phenotypes in NSCLC.

Supplementary Material

Refer to Web version on PubMed Central for supplementary material.

Acknowledgments

We thank Nam K. Yoon, Lily Zhang, Samson Schatz, and Leslie Chen for technical assistance.

Grant support: Specialized Programs of Research Excellence (SPORE) in Lung Cancer Grant P50-CA90388, NCI; LUNGevity/Thoracic Surgery Foundation for Research and Education (TSFRE) Research Fellowship; UCLA Pulmonary & Critical Care Training Grant, NIH/NHLBI T32 HL72752; Department of Veteran Affairs Medical Research Funds; Tobacco Related Disease Program Award Program of the University of California; Reiss Family and Piansky Family Trust; and the Early Detection Research Network, NCI CA-86366.

References

1. Jemal A, Siegel R, Ward E, et al. Cancer statistics, 2008. CA Cancer J Clin 2008;58:71–96. [PubMed: 18287387]
2. Peinado H, Olmeda D, Cano A. Snail, Zeb and bHLH factors in tumour progression: an alliance against the epithelial phenotype? Nat Rev Cancer 2007;7:415–28. [PubMed: 17508028]
3. Cano A, Perez-Moreno MA, Rodrigo I, et al. The transcription factor snail controls epithelial-mesenchymal transitions by repressing E-cadherin expression. Nat Cell Biol 2000;2:76–83. [PubMed: 10655586]
4. Thiery JP. Epithelial-mesenchymal transitions in tumour progression. Nat Rev Cancer 2002;2:442–54. [PubMed: 12189386]
5. Jeanes A, Gottardi CJ, Yap AS. Cadherins and cancer: how does cadherin dysfunction promote tumor progression? Oncogene 2008;27:6920–9. [PubMed: 19029934]
6. Usami Y, Satake S, Nakayama F, et al. Snail-associated epithelial-mesenchymal transition promotes oesophageal squamous cell carcinoma motility and progression. J Pathol 2008;215:330–9. [PubMed: 18491351]
7. Sun L, Diamond ME, Ottaviano AJ, Joseph MJ, Ananthanarayan V, Munshi HG. Transforming growth factor-beta 1 promotes matrix metalloproteinase-9-mediated oral cancer invasion through snail expression. Mol Cancer Res 2008;6:10–20. [PubMed: 18234959]
8. Olmeda D, Moreno-Bueno G, Flores JM, Fabra A, Portillo F, Cano A. SNAI1 is required for tumor growth and lymph node metastasis of human breast carcinoma MDA-MB-231 cells. Cancer Res 2007;67:11721–31. [PubMed: 18089802]
9. Miyoshi A, Kitajima Y, Kido S, et al. Snail accelerates cancer invasion by upregulating MMP expression and is associated with poor prognosis of hepatocellular carcinoma. Br J Cancer 2005;92:252–8. [PubMed: 15668718]
10. Kudo-Saito C, Shirako H, Takeuchi T, Kawakami Y. Cancer metastasis is accelerated through immunosuppression during Snail-induced EMT of cancer cells. Cancer Cell 2009;15:195–206. [PubMed: 19249678]
11. Barrallo-Gimeno A, Nieto MA. The Snail genes as inducers of cell movement and survival: implications in development and cancer. Development 2005;132:3151–61. [PubMed: 15983400]
12. Moody SE, Perez D, Pan TC, et al. The transcriptional repressor Snail promotes mammary tumor recurrence. Cancer Cell 2005;8:197–209. [PubMed: 16169465]
13. Escriva M, Peiro S, Herranz N, et al. Repression of PTEN phosphatase by Snail1 transcriptional factor during gamma radiation-induced apoptosis. Mol Cell Biol 2008;28:1528–40. [PubMed: 18172008]

14. Yin T, Wang C, Liu T, Zhao G, Zha Y, Yang M. Expression of snail in pancreatic cancer promotes metastasis and chemoresistance. J Surg Res 2007;141:196–203. [PubMed: 17583745]
15. Palmer HG, Larriba MJ, Garcia JM, et al. The transcription factor SNAIL represses vitamin D receptor expression and responsiveness in human colon cancer. Nat Med 2004;10:917–9. [PubMed: 15322538]
16. Dohadwala M, Yang SC, Luo J, et al. Cyclooxygenase-2-dependent regulation of E-cadherin: prostaglandin E(2) induces transcriptional repressors ZEB1 and snail in non-small cell lung cancer. Cancer Res 2006;66:5338–45. [PubMed: 16707460]
17. Zhuo W, Wang Y, Zhuo X, Zhang Y, Ao X, Chen Z. Knockdown of Snail, a novel zinc finger transcription factor, via RNA interference increases A549 cell sensitivity to cisplatin via JNK/mitochondrial pathway. Lung Cancer 2008;62:8–14. [PubMed: 18372076]
18. Mah V, Seligson DB, Li A, et al. Aromatase expression predicts survival in women with early-stage non small cell lung cancer. Cancer research 2007;67:10484–90. [PubMed: 17974992]
19. Kim HL, Seligson D, Liu X, et al. Using tumor markers to predict the survival of patients with metastatic renal cell carcinoma. J Urol 2005;173:1496–501. [PubMed: 15821467]
20. Kim HL, Seligson D, Liu X, et al. Using protein expressions to predict survival in clear cell renal carcinoma. Clin Cancer Res 2004;10:5464–71. [PubMed: 15328185]
21. Lee GY, Kenny PA, Lee EH, Bissell MJ. Three-dimensional culture models of normal and malignant breast epithelial cells. Nat Methods 2007;4:359–65. [PubMed: 17396127]
22. Li C, Wong WH. Model-based analysis of oligonucleotide arrays: expression index computation and outlier detection. Proc Natl Acad Sci U S A 2001;98:31–6. [PubMed: 11134512]
23. Breiman, L.; Friedman, JH.; Olshen, RA.; Stone, CJ. Classification and Regression Trees. Belmont, CA: Wadsworth International; 1984.
24. Moore BB, Arenberg DA, Stoy K, et al. Distinct CXC chemokines mediate tumorigenicity of prostate cancer cells. Am J Pathol 1999;154:1503–12. [PubMed: 10329603]
25. Sun H, Chung WC, Ryu SH, et al. Cyclic AMP-responsive element binding protein-and nuclear factor-kappaB-regulated CXC chemokine gene expression in lung carcinogenesis. Cancer Prev Res (Phila Pa) 2008;1:316–28. [PubMed: 19138976]
26. Arenberg DA, Keane MP, DiGiovine B, et al. Epithelial-neutrophil activating peptide (ENA-78) is an important angiogenic factor in non-small cell lung cancer. J Clin Invest 1998;102:465–72. [PubMed: 9691082]
27. Yuan A, Yang PC, Yu CJ, et al. Interleukin-8 messenger ribonucleic acid expression correlates with tumor progression, tumor angiogenesis, patient survival, and timing of relapse in non-small-cell lung cancer. Am J Respir Crit Care Med 2000;162:1957–63. [PubMed: 11069840]
28. Smith DR, Polverini PJ, Kunkel SL, et al. Inhibition of interleukin 8 attenuates angiogenesis in bronchogenic carcinoma. J Exp Med 1994;179:1409–15. [PubMed: 7513008]
29. Fontanini G, Lucchi M, Vignati S, et al. Angiogenesis as a prognostic indicator of survival in non-small-cell lung carcinoma: a prospective study. J Natl Cancer Inst 1997;89:881–6. [PubMed: 9196255]
30. Bremnes RM, Veve R, Gabrielson E, et al. High-throughput tissue microarray analysis used to evaluate biology and prognostic significance of the E-cadherin pathway in non-small-cell lung cancer. J Clin Oncol 2002;20:2417–28. [PubMed: 12011119]
31. Zhou BP, Deng J, Xia W, et al. Dual regulation of Snail by GSK-3beta-mediated phosphorylation in control of epithelial-mesenchymal transition. Nat Cell Biol 2004;6:931–40. [PubMed: 15448698]
32. Wu Y, Deng J, Rychahou PG, Qiu S, Evers BM, Zhou BP. Stabilization of snail by NF-kappaB is required for inflammation-induced cell migration and invasion. Cancer Cell 2009;15:416–28. [PubMed: 19411070]
33. Franci C, Takkunen M, Dave N, et al. Expression of Snail protein in tumor-stroma interface. Oncogene 2006;25:5134–44. [PubMed: 16568079]
34. Sanchez-Garcia I. The crossroads of oncogenesis and metastasis. N Engl J Med 2009;360:297–9. [PubMed: 19144947]
35. Rosivatz E, Becker KF, Kremmer E, et al. Expression and nuclear localization of Snail, an E-cadherin repressor, in adenocarcinomas of the upper gastrointestinal tract. Virchows Arch 2006;448:277–87. [PubMed: 16328348]

36. Come C, Magnino F, Bibeau F, et al. Snail and slug play distinct roles during breast carcinoma progression. Clin Cancer Res 2006;12:5395–402. [PubMed: 17000672]
37. Witta SE, Gemmill RM, Hirsch FR, et al. Restoring E-cadherin expression increases sensitivity to epidermal growth factor receptor inhibitors in lung cancer cell lines. Cancer Res 2006;66:944–50. [PubMed: 16424029]
38. Shih JY, Tsai MF, Chang TH, et al. Transcription repressor slug promotes carcinoma invasion and predicts outcome of patients with lung adenocarcinoma. Clin Cancer Res 2005;11:8070–8. [PubMed: 16299238]
39. Langer EM, Feng Y, Zhaoyuan H, Rauscher FJ 3rd, Kroll KL, Longmore GD. Ajuba LIM proteins are snail/slug corepressors required for neural crest development in Xenopus. Dev Cell 2008;14:424–36. [PubMed: 18331720]
40. Mejlvang J, Kriajevska M, Vandewalle C, et al. Direct repression of cyclin D1 by SIP1 attenuates cell cycle progression in cells undergoing an epithelial mesenchymal transition. Mol Biol Cell 2007;18:4615–24. [PubMed: 17855508]
41. Hu CT, Wu JR, Chang TY, Cheng CC, Wu WS. The transcriptional factor Snail simultaneously triggers cell cycle arrest and migration of human hepatoma HepG2. J Biomed Sci 2008;15:343–55. [PubMed: 18183498]
42. Bergers G, Benjamin LE. Tumorigenesis and the angiogenic switch. Nat Rev Cancer 2003;3:401–10. [PubMed: 12778130]
43. Strieter RM. Out of the shadows: CXC chemokines in promoting aberrant lung cancer angiogenesis. Cancer Prev Res (Phila Pa) 2008;1:305–7. [PubMed: 19129922]
44. Arenberg DA, Kunkel SL, Polverini PJ, Glass M, Burdick MD, Strieter RM. Inhibition of interleukin-8 reduces tumorigenesis of human non-small cell lung cancer in SCID mice. J Clin Invest 1996;97:2792–802. [PubMed: 8675690]
45. Keane MP, Belperio JA, Xue YY, Burdick MD, Strieter RM. Depletion of CXCR2 inhibits tumor growth and angiogenesis in a murine model of lung cancer. J Immunol 2004;172:2853–60. [PubMed: 14978086]
46. Wislez M, Fujimoto N, Izzo JG, et al. High expression of ligands for chemokine receptor CXCR2 in alveolar epithelial neoplasia induced by oncogenic kras. Cancer Res 2006;66:4198–207. [PubMed: 16618742]
47. Mizukami Y, Jo WS, Duerr EM, et al. Induction of interleukin-8 preserves the angiogenic response in HIF-1alpha-deficient colon cancer cells. Nat Med 2005;11:992–7. [PubMed: 16127434]
48. Martin D, Galisteo R, Gutkind JS. CXCL8/IL8 stimulates vascular endothelial growth factor (VEGF) expression and the autocrine activation of VEGFR2 in endothelial cells by activating NFkappaB through the CBM (Carma3/Bcl10/Malt1) complex. J Biol Chem 2009;284:6038–42. [PubMed: 19112107]
49. Schultheis AM, Lurje G, Rhodes KE, et al. Polymorphisms and clinical outcome in recurrent ovarian cancer treated with cyclophosphamide and bevacizumab. Clin Cancer Res 2008;14:7554–63. [PubMed: 19010874]
50. Zhang, W.; Dahlberg, SE.; Yang, D., et al. Genetic variants in angiogenesis pathway associated with clinical outcome in NSCLC patients (pts) treated with bevacizumab in combination with carboplatin and paclitaxel: Subset pharmacogenetic analysis of EGOG 4599. J Clin Oncol; 2009 ASCO Annual Meeting; 2009. suppl; abstr 8032

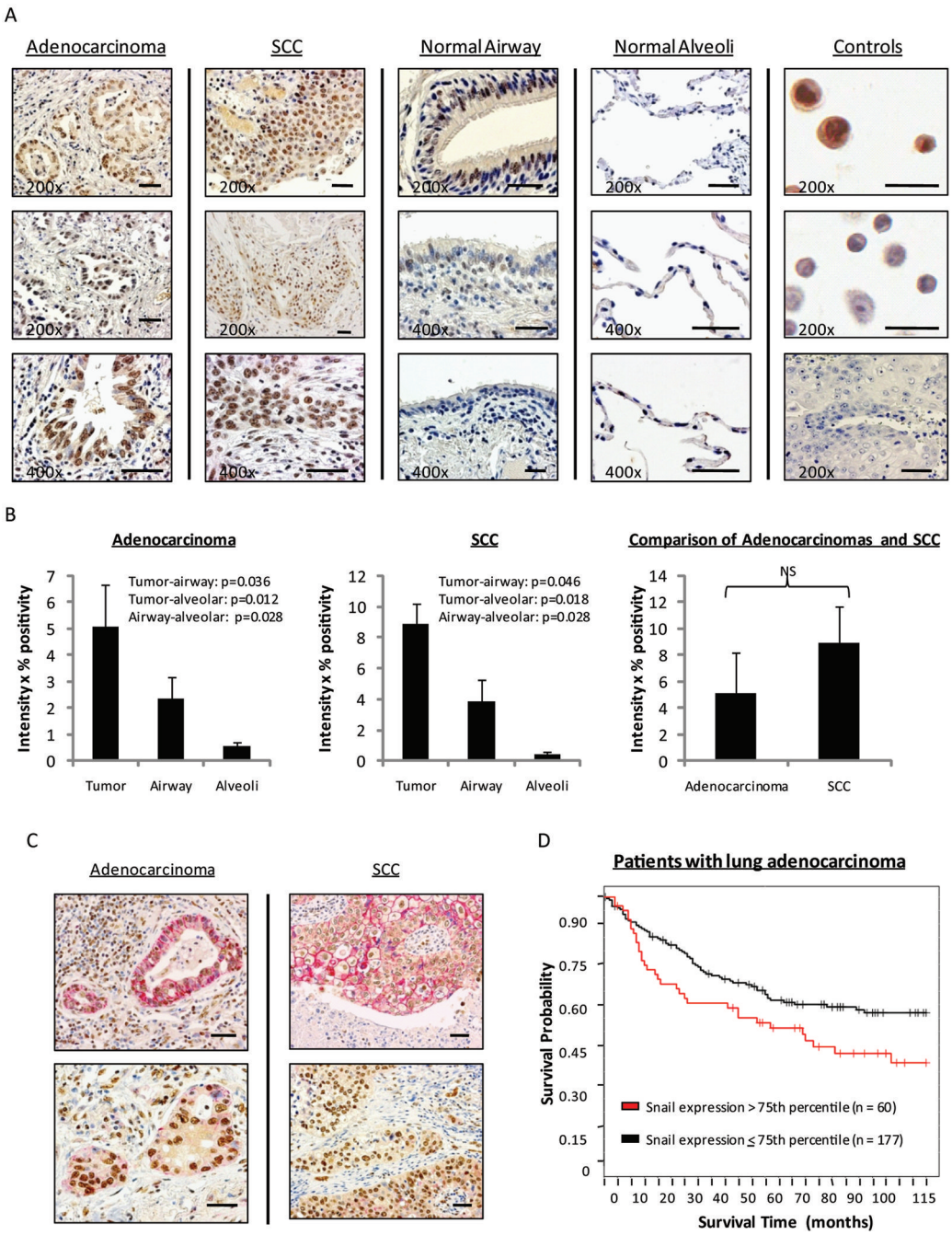

Figure 1.

Snail is up-regulated in human NSCLC tissues and correlates with decreased survival. *A*, Sections of human NSCLC tissues with brown nuclear Snail staining. In the column of controls, *top* image depicts Snail staining of a paraffin-embedded pellet of Snail over-expressing cells (positive control). *Middle* image represents Snail staining of a paraffin-embedded pellet of vector control cells (negative control). *Bottom* image is human NSCLC tissue, serving as a negative isotype control. *B*, Evaluation of Snail levels in tumor tissues as well as surrounding normal airway and alveolar epithelium. NS = not statistically significant. Error bars represent standard error (SE), except for comparison of adenocarcinomas versus SCCs, where error bars represent 2SE. *C*, Red membranous E-cadherin and brown nuclear Snail staining in NSCLC

tissues, reflecting non-uniform expression of E-cadherin in the presence of Snail. *D*, TMA analysis of survival as related to levels of tumor Snail expression, represented by Kaplan-Meier plot. ($p<0.026$)

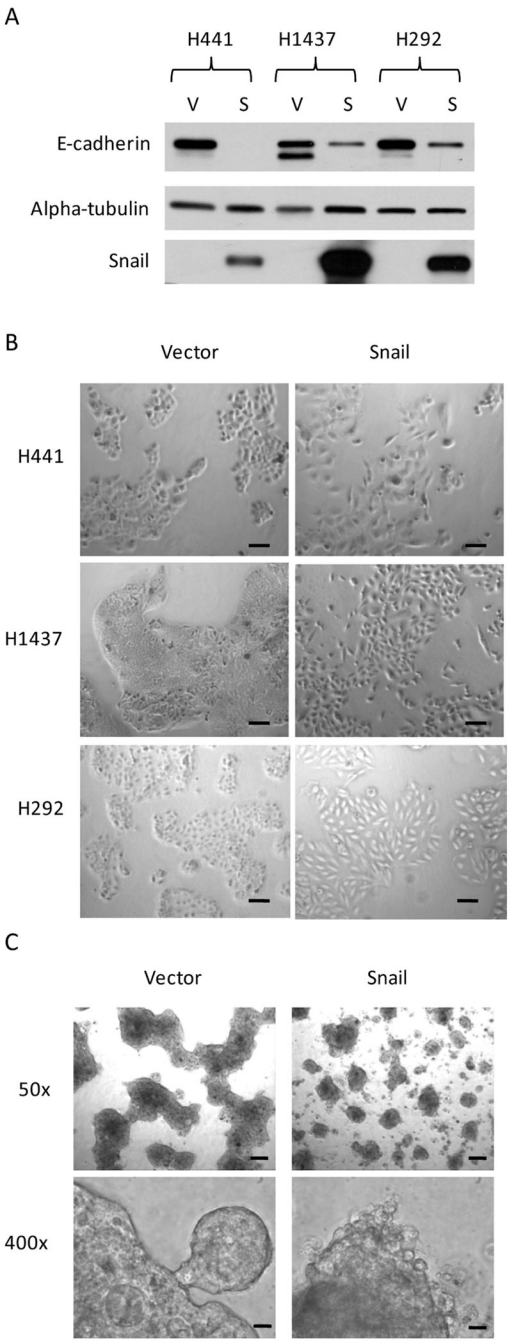

Figure 2.

Snail over-expression leads to morphologic changes in NSCLC cell lines. *A*, Western blot analysis verifies the up-regulation of Snail, with concomitant down-regulation of E-cadherin, in NSCLC cell lines stably transduced to over-express Snail. Equal loading of protein obtained from whole-cell lysates was confirmed with an anti-alpha-tubulin antibody. (Full-length blots presented in Supplemental Figure 2.) *B*, Cells grown in traditional two-dimensional culture. Images obtained at 50x original magnification. Scale bars represent 100 μm. *C*, Cells cultured for 14 days in a three-dimensional spheroid culture model. Photographs taken at 50x or 400x original magnification, as labeled in figure. Scale bars for photos taken at original

magnification 50x are 200 μm, whereas scale bars for photos taken at original magnification 400x are 20 μm.

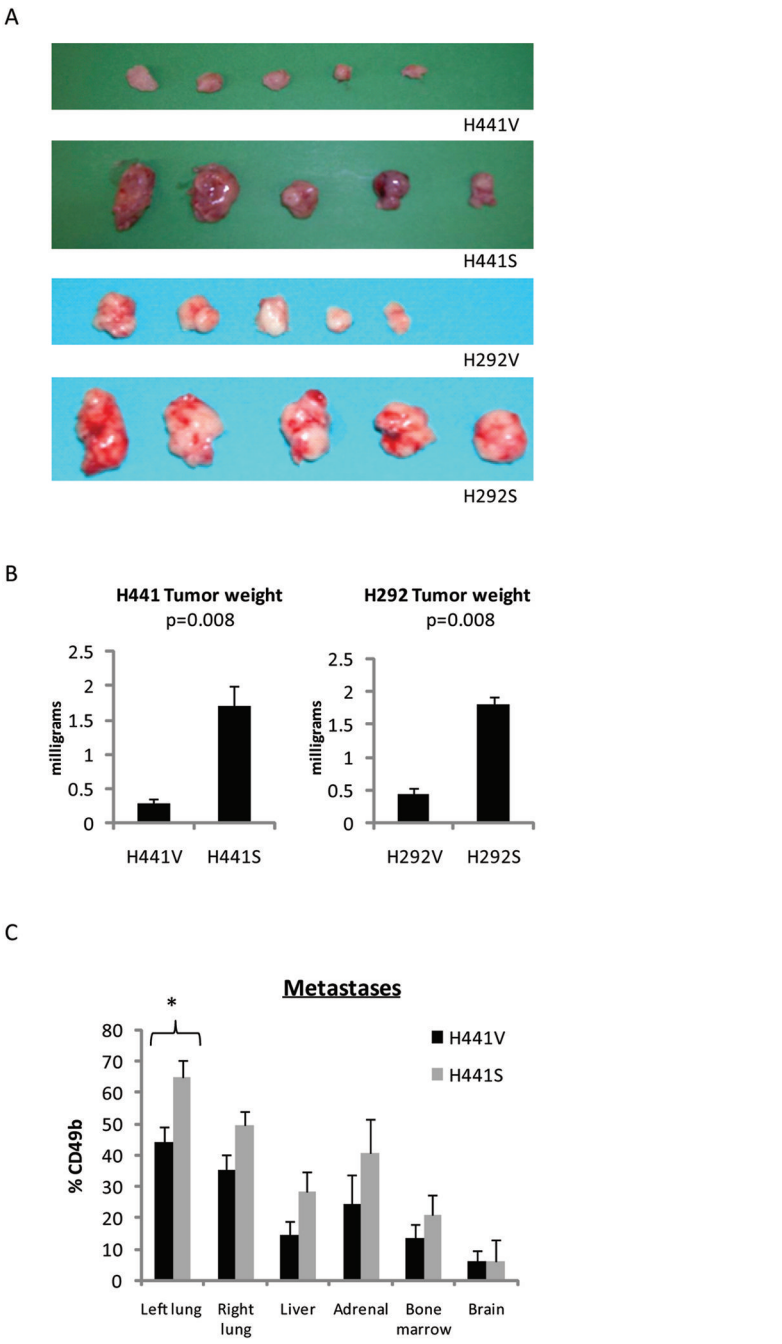

Figure 3.

Snail over-expression leads to increased NSCLC tumor growth *in vivo*. *A*, For the heterotopic model, primary tumors were harvested after 6 weeks of growth. (5 mice/group). (p=0.008) *B*, Photograph of tumors. *C*, For the orthotopic model, organs were harvested after 10 weeks of growth (5 mice/group) and evaluated by flow cytometry gated on the human marker, CD49b. (p=0.025 for the primary tumor site, >0.05 for all other sites). Error bars represent SE.

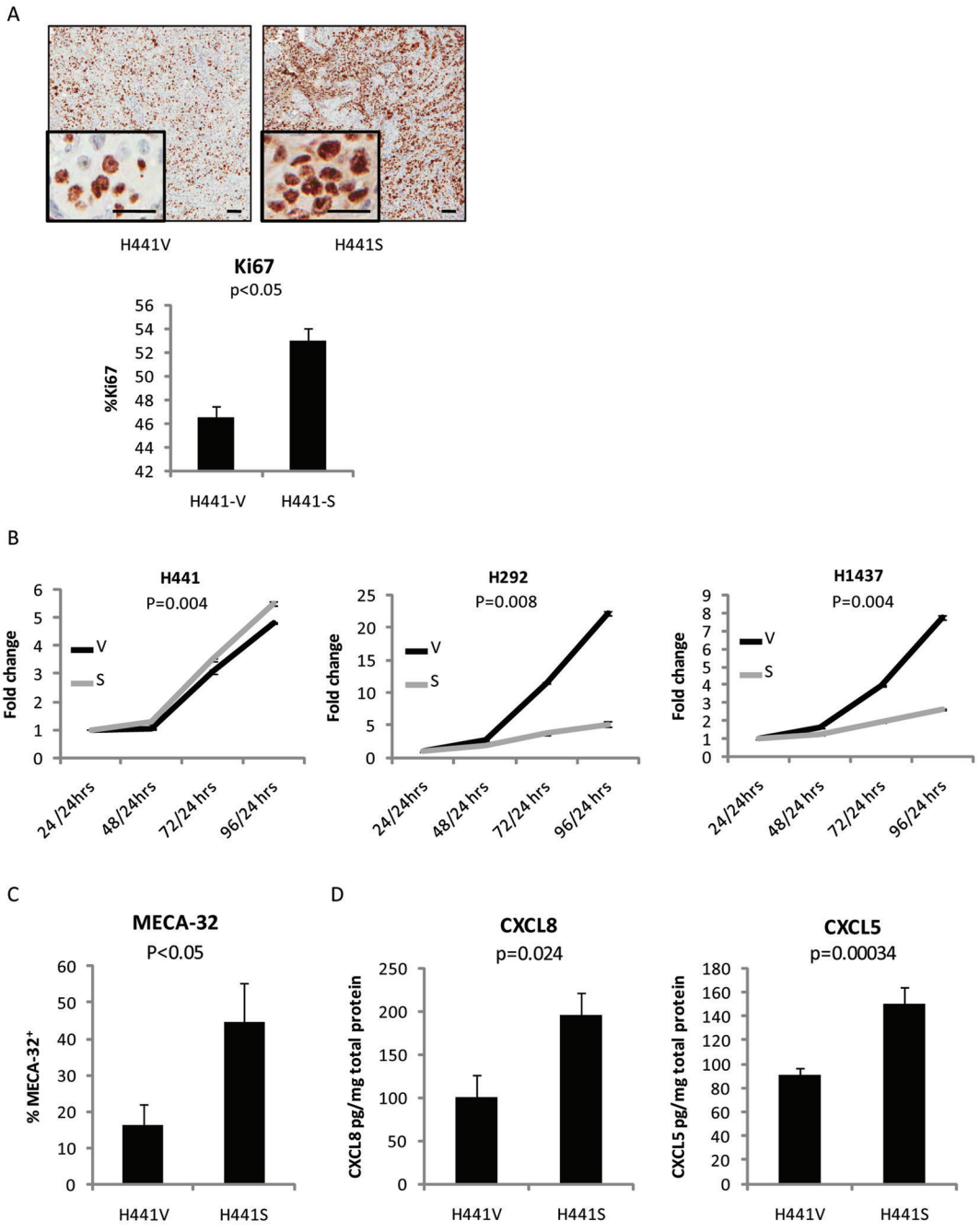

Figure 4.

Snail over-expression leads to increased angiogenesis and elevated levels of angiogenic factors *in vivo*. *A*, Tumors harvested from the heterotopic model were evaluated for a proliferation marker, Ki67 (4 mice/group). Representative images at 20x with inset 200x magnification. Scale bars for 20x photos equal 100 μm, while scale bars for 200x images represent 25 μm. Staining results were quantified using the Ariol system. *B*, Luminescence assay of *in vitro* cells depicts proliferation rates. Results represented in terms of fold change in luminescent signal over time. *C*, Using the heterotopic model, after 4 weeks of growth, resultant primary tumors were analyzed by flow cytometry gated on the mouse endothelial cell marker, MECA-32 (7

mice/group). ($p<0.05$) *D*, Primary tumor homogenates were analyzed by ELISA for levels of two angiogenic factors: CXCL8 and CXCL5. (12 mice/group) Error bars equal SE.

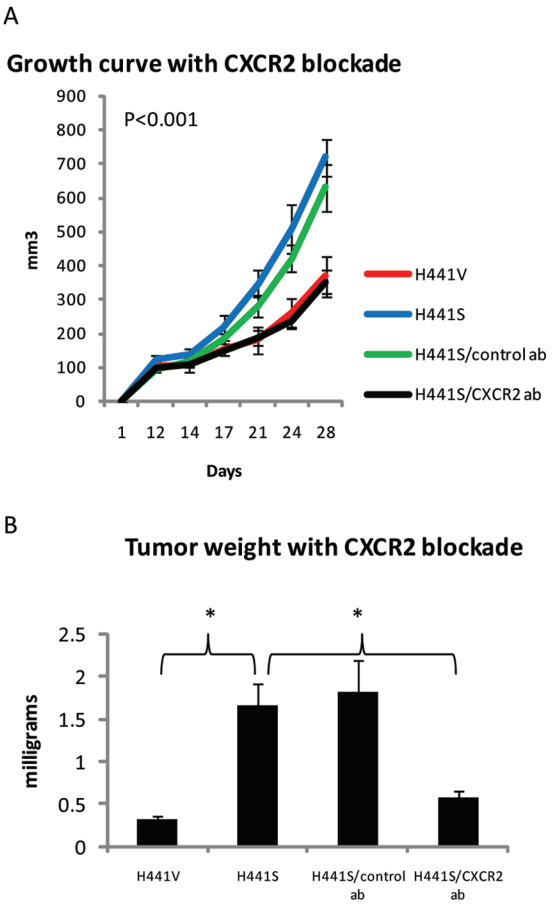

Figure 5.

Snail-dependent tumor growth is abrogated with CXCR2 blockade. Using the heterotopic model, mice were inoculated with either H441V or H441S cells. Mice bearing H441S tumors were divided into three groups: untreated, treated with control antibody, or treated with anti-CXCR2 antibody. *A*, Tumor growth curve during four weeks of growth (12 mice/group). *B*, Tumor weights after harvest at five weeks (4 mice/group). Error bars represent SE.

Table 1

Selected genes modified with statistical significance ($p<0.05$) for Snail over-expressing as compared to vector control NSCLC cells. (↑=up-regulation, ↓=down-regulation)

Probe set	Gene	Accession	P value
	Angiogenesis		
203002_at	angiomotin like 2 (↑)	NM_016201	0.044
210845_s_at	plasminogen activator, urokinase receptor (↑)	U08839	0.038
218520_at	TANK-binding kinase 1 (↑)	NM_013254	0.032
200628_s_at	tryptophanyl-tRNA synthetase (↑)	M61715	0.045
200677_at	pituitary tumor-transforming 1 interacting protein (↑)	NM_004339	0.029
204773_at	interleukin 11 receptor, alpha (↑)	NM_004512	0.044
227095_at	leptin receptor (↑)	AU151151	0.028
201109_s_at	thrombospondin 1 (↑)	AV726673	0.048
201110_s_at	thrombospondin 1 (↑)	NM_003246	0.048
211547_s_at	platelet-activating factor acetylhydrolase, isoform Ib, αsubunit 45kDa (↑)	L13387	0.049
201286_at	syndecan 1 (↓)	Z48199	0.04
201287_s_at	syndecan 1 (↓)	NM_002997	0.034
	Invasion and metastasis		
234001_s_at	ADP-ribosylation factor GTPase activating protein 1 (↑)	AL137744	0.034
214088_s_at	fucosyltransferase 3 (galactoside 3(4)-L-fucosyltransferase, Lewis blood group included) (↓)	AW080549	0.021
221754_s_at	coronin, actin binding protein, 1B (↓)	AI341234	0.023
	Cell cycle		
202723_s_at	forkhead box O1A (rhabdomyosarcoma) (↑)	AW117498	0.038
204604_at	PFTAIRE protein kinase 1 (↑)	NM_012395	0.034
1554408_a_at	thymidine kinase 1, soluble (↓)	BC007986	0.008
	Tumor suppressor		
213473_at	BRCA1 associated protein (↑)	AL042733	0.042
1554006_a_at	lethal giant larvae homolog 2 (Drosophila) (↓)	BC006503	0.044